# *Characterization of an atypical, thermostable, organic solvent- and acid-tolerant 2#-deoxyribosyltransferase from* Chroococcidiopsis thermalis

**Jon Del Arco, Pedro Alejandro Sánchez-Murcia, José Miguel Mancheño, Federico Gago & Jesús Fernández-Lucas**

**Applied Microbiology and Biotechnology**

ISSN 0175-7598
Volume 102
Number 16

Appl Microbiol Biotechnol (2018)
102:6947-6957
DOI 10.1007/s00253-018-9134-y


Springer

Applied Microbiology and Biotechnology (2018) 102:6947–6957
https://doi.org/10.1007/s00253-018-9134-y

BIOTECHNOLOGICALLY RELEVANT ENZYMES AND PROTEINS

# Characterization of an atypical, thermostable, organic solvent- and acid-tolerant 2′-deoxyribosyltransferase from *Chroococcidiopsis thermalis*

Jon Del Arco[1] · Pedro Alejandro Sánchez-Murcia[2] · José Miguel Mancheño[3] · Federico Gago[4] · Jesús Fernández-Lucas[1,5]

Received: 23 January 2018 / Revised: 15 May 2018 / Accepted: 23 May 2018 / Published online: 5 June 2018


## Abstract

In our search for thermophilic and acid-tolerant nucleoside 2′-deoxyribosyltransferases (NDTs), we found a good candidate in an enzyme encoded by *Chroococcidiopsis thermalis* PCC 7203 (*Ct*NDT). Biophysical and biochemical characterization revealed *Ct*NDT as a homotetramer endowed with good activity and stability at both high temperatures (50–100 °C) and a wide range of pH values (from 3 to 7). *Ct*NDT recognizes purine bases and their corresponding 2′-deoxynucleosides but is also proficient using cytosine and 2′-deoxycytidine as substrates. These unusual features preclude the strict classification of *Ct*NDT as either a type I or a type II NDT and further suggest that this simple subdivision may need to be updated in the future. Our findings also hint at a possible link between oligomeric state and NDT's substrate specificity. Interestingly from a practical perspective, *Ct*NDT displays high activity (80–100%) in the presence of several water-miscible co-solvents in a proportion of up to 20% and was successfully employed in the enzymatic production of several therapeutic nucleosides such as didanosine, vidarabine, and cytarabine.

**Keywords** Enzymatic synthesis · Nucleoside analogues · Nucleoside 2′-deoxyribosyltransferase · Extremophiles · Homology modeling

## Introduction

Nowadays, the application of bioprocesses catalyzed by whole cells or enzymes in industrial settings is gaining momentum over traditional chemical synthetic processes. In this context, the enzymatic synthesis of active pharmaceutical ingredients (APIs) shows many advantages, such as one-pot reactions under mild conditions, high stereo- and regioselectivity, and an environmentally friendly technology (Patel 2017). Nonetheless, several limitations, such as their instability and poor performance under certain reaction conditions, their high production costs, and the low solubility of some substrates in the reaction medium, must be overcome to scale up these processes from the laboratory to the manufacturing plant. To develop efficient and economical processes, the modern industry has an increasing demand for novel biocatalysts that exhibit activity and stability under a wide range of reaction conditions (e.g., extreme pH values, high temperatures, or the presence of organic solvents). In this context, enzymes from extremophiles are valuable biocatalysts for the industrial implementation of bioprocesses.

**Electronic supplementary material** The online version of this article (https://doi.org/10.1007/s00253-018-9134-y) contains supplementary material, which is available to authorized users.

✉ Jesús Fernández-Lucas
jesus.fernandez2@universidadeuropea.es

[1] Applied Biotechnology Group, Universidad Europea de Madrid, Urbanización El Bosque, c/ Tajo, s/n, Villaviciosa de Odón, 28670 Madrid, Spain

[2] Institute of Theoretical Chemistry, Faculty of Chemistry, University of Vienna, 1090 Vienna, Austria

[3] Department of Crystallography and Structural Biology, Rocasolano Institute (CSIC), c/ Serrano 119, 28006 Madrid, Spain

[4] Department of Biomedical Sciences and "Unidad Asociada IQM-CSIC", School of Medicine and Health Sciences, University of Alcalá, Alcalá de Henares, 28805 Madrid, Spain

[5] Grupo de Investigación en Desarrollo Agroindustrial Sostenible, Universidad de la Costa, CUC, Calle 58 # 55-66, Barranquilla 080002, Colombia

Modified nucleosides are useful therapeutic agents endowed with antitumor, antiviral, and antibiotic activities (De Clercq 2005; Parker 2009). Due to their economic and social importance, the availability of stereoselective, sustainable, and cheap synthetic methods could be very valuable for the pharmaceutical industry. The enzymatic synthesis of nucleoside analogues by transglycosylation reactions is an interesting and sustainable alternative to traditional multistep chemical methods (Iglesias et al. 2015; Lapponi et al. 2016; Mikhailopulo 2007). In this regard, nucleoside 2′-deoxyribosyltransferases (NDTs) (Fresco-Taboada et al. 2013), nucleoside phosphorylases (Lewkowicz and Iribarren 2006), and some nucleoside hydrolases (Mitsukawa et al. 2017) have been used as valuable catalysts in the synthesis of many different modified nucleosides.

NDTs (EC: 2.4.2.6) catalyze the exchange of the 2′-deoxyribose moiety between purine and/or pyrimidine bases (Fig. 1) (Crespo et al. 2017; Fresco-Taboada et al. 2013). Traditionally, according to their substrate specificity, NDTs are classified as type I (PDT), specific for purines (Pur ↔ Pur), or type II (NDT), which catalyze the transfer between purines and/or pyrimidines (Pur ↔ Pur, Pur ↔ Pyr, Pyr ↔ Pyr) (Fresco-Taboada et al. 2013; Kaminski 2002). NDTs are highly specific for 2′-deoxyribonucleosides, as well as regioselective (N1 glycosylation in pyrimidines and N9 in purines) and stereoselective (β-anomers are exclusively formed). These enzymes are very tolerant to nucleobase modifications, and numerous examples of enzymatic synthesis of nucleoside analogues using modified bases have been reported in the literature (Britos et al. 2016; Fernández-Lucas et al. 2012; Fresco-Taboada et al. 2013; Vichier-Guerre et al. 2016). In addition, despite their extreme specificity over 2′-deoxyribonucleosides, recent studies have shown that some NDTs can recognize modified 2′C and 3′C nucleosides to some extent (Crespo et al. 2017; Fernández-Lucas et al. 2010; Fresco-Taboada et al. 2013; Kaminski et al. 2008).

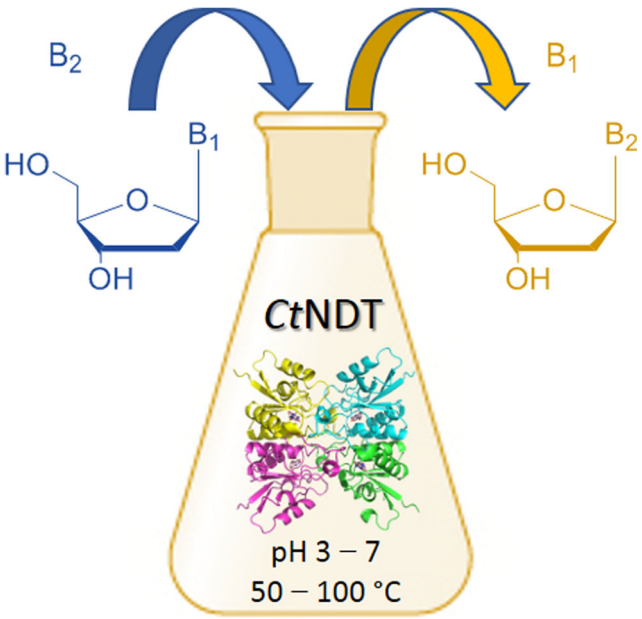


**Fig. 1** Transglycosylation reaction catalyzed by *Ct*NDT

The present work aimed to identify an NDT with the ability to act as a biocatalyst for the synthesis of natural and nonnatural nucleosides under extreme conditions. We now report, for the first time to the best of our knowledge, the cloning of the *ndt* gene from *Chroococcidiopsis thermalis* PCC 7203, its expression in *Escherichia coli*, and the purification of the recombinant protein (*Ct*NDT), which has been characterized by biophysical and biochemical methods. Furthermore, we have tested the activity of *Ct*NDT in the presence of up to 20% of several water-miscible co-solvents and explored its potential as an industrial biocatalyst for the enzymatic production of different therapeutic nucleosides such as didanosine (2′,3′-dideoxyinosine, ddI), vidarabine (arabinosil adenine, ara-A), and cytarabine (arabinosil cytosine, ara-C).

## Materials and methods

### Materials

Cell culture medium reagents were from Difco (St. Louis, USA). Trimethyl ammonium acetate buffer was purchased from Sigma-Aldrich (Madrid, Spain). All other reagents and organic solvents were purchased from Scharlab (Barcelona, Spain) and Symta (Madrid, Spain). Nucleosides and nucleobases used in this work were provided by Carbosynth Ltd. (Compton, UK).

### Gene expression and protein purification

The *ndt* gene, which encodes a protein annotated as a nucleoside 2′-deoxyribosyltransferase from *Chroococcidiopsis thermalis* PCC 7203 (European Nucleotide Archive code: AFY86715.1; UniProtKB code K9TVX3), was purchased from GenScript (USA). The coding sequence appeared as a *Nde*I-*Eco*RI fragment subcloned into the expression vector pET28b (+). The resultant, recombinant vector pET28b*Ct*NDT provided an N-terminal $His_6$-tagged fusion with a thrombin cleavage site between the tag and the enzyme. *Ct*NDT was expressed in *E. coli* BL21(DE3) grown at 37 °C in LB medium containing kanamycin 50 μg/mL. Protein overexpression was induced by adding 0.5 mM isopropyl β-D-1-thiogalactopyranoside and the cells were further grown for 3 h. Cells were harvested by centrifugation at 3500×*g* and the resulting pellet was resuspended in 10 mM sodium phosphate buffer pH 7. Crude extracts were prepared by French press lysis of cell suspensions. The lysate was centrifuged at 17,500×*g* for 30 min and the supernatant was filtered through a 0.22-μm filter (Millipore). The cleared lysate was loaded onto a 5-mL HisTrap FF column (GE Healthcare)

pre-equilibrated in a binding buffer (20 mM Tris-HCl buffer, pH 8.0, with 100 mM NaCl and 10 mM imidazole) and the column was washed. Bound proteins were eluted using a linear gradient of imidazole (from 10 to 500 mM). Fractions containing *Ct*NDT were identified by SDS-PAGE, pooled, concentrated, and loaded onto a HiLoad 16/60 Superdex 200 prep grade column (GE Healthcare) pre-equilibrated in 50 mM sodium phosphate, pH 7.0. Fractions with the protein of interest identified by SDS-PAGE were pooled, and the protein was dialyzed against 10 mM sodium phosphate, pH 7.0, and concentrated and stored at 4 °C until its use. Electrophoresis was carried out on a 15% polyacrylamide slab gel with 25 mM Tris-HCl buffer, pH 8.6, 0.1% SDS (Laemmli 1970). Protein concentration was determined spectrophotometrically by UV absorption at 280 nm using $\varepsilon_{280} = 8940\ M^{-1}\ cm^{-1}$ (Gill and von Hippel 1989).

## Analytical ultracentrifugation analysis

Sedimentation velocity experiments for *Ct*NDT were carried out in 10 mM sodium phosphate (pH 8.0, 20 °C, 50,000×*g*) using an Optima XL-I analytical ultracentrifuge (Beckman-Coulter Inc.) equipped with UV-VIS absorbance and Raleigh interference detection systems, using an An-60Ti rotor and standard (12 mm optical path) double-sector center pieces of Epon charcoal. Sedimentation profiles were recorded at 292 nm. Sedimentation coefficient distributions were calculated by least-squares boundary modeling of sedimentation velocity using the continuous distribution *c*(*s*) Lamm equation model as implemented in SEDFIT 14.7g (Brown and Schuck 2006; https://sedfitsedphat.nibib.nih.gov/software/default.aspx). Baseline offsets were measured afterwards at 200,000×*g*. The experimental sedimentation coefficients were corrected to standard conditions (water, 20 °C, and infinite dilution) using SEDNTERP software to obtain the corresponding standard values ($s_{20,w}$) (Van Holde 1985).

## Enzyme activity assay

The standard activity assay was performed by incubating 0.6 μg of pure enzyme with 10 mM 2′-deoxyinosine (dIno) and 10 mM adenine in 50 mM MES buffer pH 6.0 in a final volume of 40 μL. The reaction mixture was incubated at 40 °C for 10 min (300 rpm). The enzyme was inactivated by adding 40 μL of cold methanol in an ice bath and heating for 5 min at 100 °C. After centrifugation at 9000×*g* for 2 min, the samples were half-diluted with water and frozen at − 20 °C. Nucleotide production was analyzed using HPLC to measure the reaction products quantitatively, as described below. All determinations were carried out in triplicate and the maximum error was less than 5%. Under such conditions, one international activity unit (IU) was defined as the amount of enzyme producing 1 μmol/min of 2′-deoxyadenosine under the assay conditions.

## Influence of pH and temperature on enzyme activity

The pH profile of purified recombinant enzyme was initially determined using the standard assay, as described above, with sodium citrate (pH 4–6), sodium phosphate (pH 6–8), and sodium borate (pH 8–10) as reaction buffers (50 mM). The optimum temperature was determined using the standard assay across a 20–90 °C range.

## Thermal and pH stability of *Ct*NDT

*Ct*NDT was stored at 4 °C in 10 mM sodium phosphate, pH 7.0 for 135 days. Samples were taken periodically for enzymatic activity evaluation. Storage stability was defined as the relative activity between the first and successive reactions. Moreover, the thermal stability of *Ct*NDT was assessed by incubating 0.3 μg of pure enzyme in a pH range from 5 to 7, at 60 °C for a period of 140 h. After this, the activity was measured using the standard assay.

## Enzymatic activity in nonconventional media

To determine the influence of water-miscible organic solvents on *Ct*NDT activity, the synthesis of 2′-deoxyadenosine from 2′-deoxyinosine and adenine was tested under the standard assay conditions in the presence of 20% water-miscible organic solvents.

## Enzymatic production nucleoside analogues

The enzymatic syntheses of different nucleoside analogues were performed by incubating 3.75 μg of pure enzyme with 1 mM purine base and 1 mM nucleoside analogues in different reaction buffers (pH 6.0 and 8.5) in a final volume of 40 μL. The reaction mixtures were incubated at 60 °C and 300 rpm in an orbital shaker for different reaction times (1–24 h).

## Homology modeling

The *Ct*NDT amino acid sequence (UNIPROT code K9TVX3) was aligned against the UniProtKB sequences using the Basic Local Alignment Search Tool (BLAST) (http://www.uniprot.org/blast) and SANSparallel (Somervuo and Holm 2015). A variety of 3D structural models of a *Ct*NDT homodimer were built using the threading methods implemented in the Phyre2.0 (Kelley et al. 2015) and Swiss-Model (Biasini et al. 2014) servers. The best protein templates of known 3D structure were the NDTs from *Trypanosoma brucei*, *Lactobacillus helveticus*, and *Leishmania mexicana* (PDB entries 2A0K, 1S2D, and 5NBR, respectively); a conserved protein from *Enterococcus faecalis* v583 (PDB entry 3EHD); and the CMP *N*-glycosidase MilB from *Streptomyces rimofaciens* (PDB entry 4JEM), the only enzyme in this group in which

all of the interactions necessary for catalysis are thought to occur within a single monomer (Sikowitz et al. 2013), even though the hydrophobic side chains of Phe126# and Leu127# contribute to binding of the cytosine ring. Approximately 94% of residues of *Ct*NDT (1–145) could thus be modeled at > 90% confidence. Noteworthy, none of these models by itself provided full consistency, and we found it necessary to make a composite using the information derived from the MSA carried out on NDT structural neighbors by the updated Dali server (Holm and Laakso 2016) (Fig. S1). Furthermore, the amino acid stretches 41–55 and 116–133 in both subunits were modeled with the aid of the random coordinate descent (RCD) loop closure algorithm (López-Blanco et al. 2016), which refines the top-ranking solutions with the Rosetta energy function (Alford et al. 2017). For substrate positioning inside the active site, use was made of the crystal structures of type I NDT from *L. helveticus* (*Lh*PDT) in complex with 2′-deoxyadenosine or forming a ribosylated enzyme intermediate (PDB codes 1S2G and 1S2D, respectively) (Anand et al. 2004), type II NDT from *Lactobacillus leichmannii* (*Ll*NDT) in complex with the noncleavable substrate analogue 5-methyl-2′-deoxypseudouridine (PDB code 1F8Y) (Armstrong et al. 1996), and MilB from *Streptomyces rimofaciens* in complex with cytidine 5′-monophosphate (CMP) (PDB entry 4JEM) (Sikowitz et al. 2013). PyMOL was used for structure visualization, molecular editing, and figure preparation (DeLano 2013). The AMBER force field (Case et al. 2015) was used for progressive energy refinement in explicit solvent (Salomon-Ferrer et al. 2013) following a previously described protocol (Oliva et al. 2017).

### Analytical methods

Nucleoside production was analyzed quantitatively with an ACE 5-μm C18-PFP 250-mm × 46-mm column (Advanced Chromatography Technologies) pre-equilibrated in 100% trimethyl ammonium acetate. Elution was carried out by a discontinuous gradient, 0–15 min, 100 to 90% trimethyl ammonium acetate and 0 to 10% acetonitrile, and 10–20 min, 90 to 100% trimethyl ammonium acetate and 10 to 0% acetonitrile. Retention times for the reference natural compounds (hereafter abbreviated according to the recommendations of the IUPAC-IUB Commission on Biochemical Nomenclature) were as follows: adenine (Ade), 10.14 min; 2′-deoxyadenosine (dAdo), 15.50 min; cytosine (Cyt), 4.8 min; 2′-deoxycytidine (dCyd), 8.3 min; guanine (Gua), 8.1 min; 2′-deoxyguanosine (dGuo), 12.8 min; hypoxanthine (Hyp), 7.5 min; 2′-deoxyinosine (dIno), 12.1 min; thymine (Thy), 10.0 min; 2′-deoxythymidine (dThd), 13.5 min; uracil (Ura), 5.6 min; and 2′-deoxyuridine (dUri), 9.6 min. Retention times for the reference nonnatural compounds were as follows: arabinosyl-adenine (ara-A), 14.0 min; arabinosyl-cytosine (ara-C), 8.0 min; arabinosyl-guanine (ara-G), 11.4 min; arabinosyl-hypoxanthine (ara-H), 11.0 min; 2′-deoxy-2′-fluoroadenosine (2′dFAdo), 17.0 min; 2′-deoxy-2′-fluorocytidine (2′dFCyd), 9.05 min; 2′-deoxy-2′-fluoroguanosine (2′dFGuo), 13.6 min; 2′-deoxy-2′-fluoroinosine (2′dFIno), 13.3 min; 2′,3′-dideoxyadenosine (ddA), 19.0 min; 2′,3′-dideoxycytidine (ddC), 12.3 min; 2′,3′-dideoxyguanosine (ddG), 15.3 min; and 2′,3′-dideoxyinosine (ddI), 14.8 min. To confirm the reaction products, commercial nucleoside analogues were used as HPLC standards.

## Results

### Bioinformatic analysis of the gene encoding a nucleoside 2′-deoxyribosyltransferase from *Chroococcidiopsis thermalis* PCC 7203

Sequencing of the complete genome of *Chroococcidiopsis thermalis* PCC 7203 (NCBI Reference Sequence: NC_019695) displayed one ORF (*CHRO_RS05855*, *ndt* gene) annotated as a putative NDT. This ORF was subjected to bioinformatic analyses to identify the biophysical and biochemical properties and possible 3D structure of the encoded protein. A BLAST analysis revealed that the *ndt* gene could indeed code for a putative NDT. A multiple sequence alignment (MSA) performed with SANSparallel (Somervuo and Holm 2015) confirmed that *Ct*NDT displays < 35% sequence identity with other well-studied family members, such as the NDTs from *Lactobacillus reuteri*, *Lr*NDT (34%) (Fernández-Lucas et al. 2010); *Lactobacillus fermentum*, *Lf*NDT (31%) (Kaminski et al. 2008); *Lactobacillus leichmannii*, *Ll*NDT (30%) (Cook et al. 1990); *Leishmania mexicana*, *Lm*PDT (29%) (Crespo et al. 2017); *Borrelia burgdorferi*, *Bb*PDT (29%) (Lawrence et al. 2009); and *Lactobacillus helveticus*, *Lh*PDT (26%) (Kaminski 2002). The N-terminal $His_6$-tagged *Ct*NDT was predicted by ProtParam (http://web.expasy.org/protparam) to contain 171 amino acid residues and have a relative molecular mass of 19.60 kDa.

Most important in the MSA was the finding that the canonical catalytic residues identified in NDTs from other bacteria and protozoans characterized so far are fully conserved in *Ct*NDT (Fig. S1), strongly suggesting a similarly structured active site that requires the participation of side chains from, at least, two subunits (Figs. 2 and 3). Thus, *Ct*NDT displays the typical 2′-deoxyribose-binding site motif, made up of three acidic residues from one subunit (Asp62, Asp82, Glu88) and one polar residue from the neighboring subunit in the dimer (Asn118#), which together constitute a hydrophilic core that is common to both NDT types. However, the bioinformatic analysis of the *Ct*NDT amino acid sequence could not provide evidence about the nature of the binding site for the heteroaromatic base, and it was not possible to predict in silico whether *Ct*NDT is a type I or a type II NDT. As reported in the literature (Crespo et al. 2017; Fresco-Taboada et al. 2013;

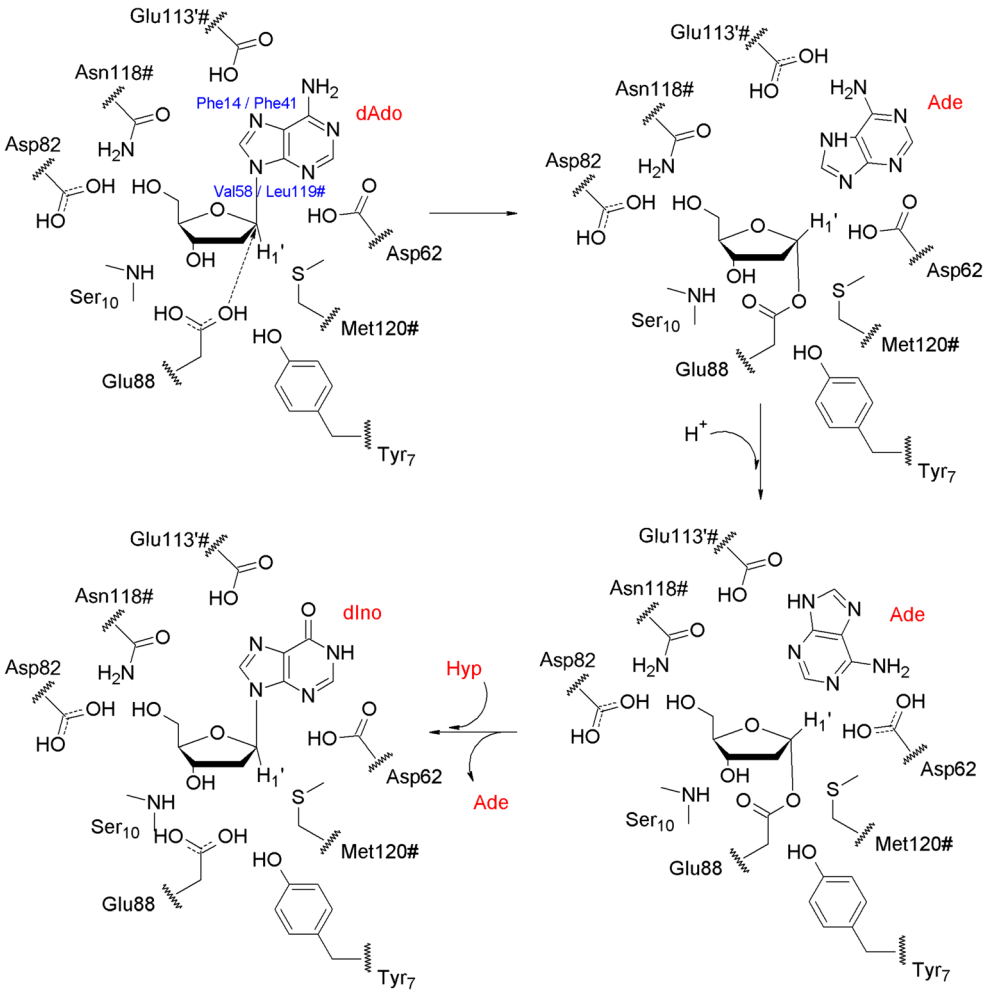


**Fig. 2** Reaction carried out by *Ct*NDT and residues involved in substrate positioning and catalysis. dAdo was used as an example of nucleoside donor and hypoxanthine as an example of base acceptor so as to yield dIno as the final product. Asp62 from one monomer and Glu113 from another dimer (Glu113'#) are proposed to be involved in nucleobase recognition and proton shuttling

Kaminski 2002), NDTs display a promiscuous base-binding site, lined with polar and aromatic residues, which satisfies all possibilities for lax hydrogen bonding with different nucleobases. The main difference between type I and type II NDTs is the role of a conserved loop region, which can serve as an active site flap. The presence of a Gln residue in this loop region capable of hydrogen bonding to both types of nucleobases (i.e., purines and pyrimidines) was early proposed to be responsible for forcing this loop to close over the base-binding active site and shield it from the surrounding solvent (type II NDT) (Sikowitz et al. 2013). In the case of PDTs, however, it has been generally assumed that the absence of this Gln residue prevents these stabilizing interactions and results in the adoption by this loop of a more solvent-exposed conformation. Nonetheless, recent studies (Crespo et al. 2017) and experimental results reported in this work (as described below) suggest that this hypothesis should be reconsidered.

With respect to the possibility that the obligate dimer associates to form a higher-order functional structure, we have previously noted (Crespo et al. 2017) a potential connection between the length of the α3 helix in NDTs and the enzyme's oligomeric state. Since this α-helix is longer in hexameric enzymes (~20 residues) than in dimeric ones (~16 residues), the predicted length of the corresponding sequence in *Ct*NDT (14 residues) strongly suggested to us that the functional enzyme was unlikely to be a hexamer (see below).

## Production and purification of *Ct*NDT

The *ndt* gene, encoding a putative nucleoside 2′-deoxyribosyltransferase from *Chroococcidiopsis thermalis* PCC 7203, was cloned and overexpressed in *E. coli* BL21(DE3), as described above. The recombinant N-terminal $His_6$-tagged *Ct*NDT was purified using two chromatographic steps. SDS-PAGE analysis of the purified enzyme showed only one protein band with an apparent molecular mass of 19.60 kDa (Fig. S2).

Sedimentation velocity experiments revealed $His_6$-tagged *Ct*NDT as a single species with an experimental sedimentation coefficient of 4.64 S ($s_{20,w}$ = 4.68) compatible with a tetrameric state (Mw = 75.50 kDa). This value corresponds to a single-species monomeric model of 18.87 kDa, similar to the molecular mass calculated from the amino acid sequence

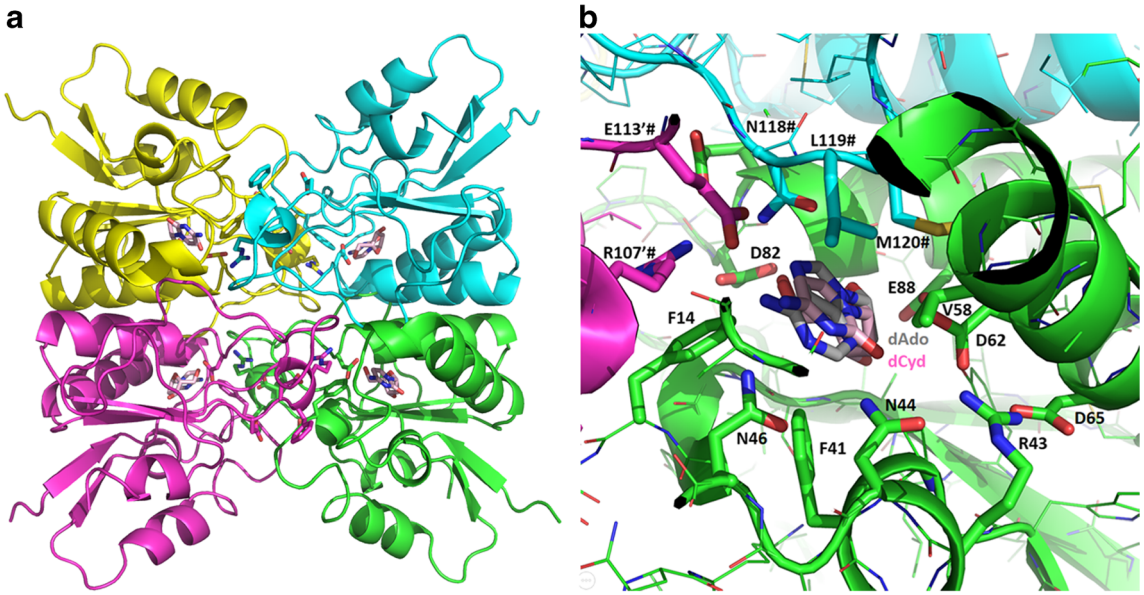


**Fig. 3** **a** Cartoon representation of a *Ct*NDT tetramer model comprising dimers A:B (green:cyan) and C:D (magenta:yellow) and a dCyd substrate (sticks) in each active site. Putative interfacial residues Phe14, Asp82, Asp105, and Arg107 are shown as sticks. **b** Close-up view of the active site region in monomer A, with residues involved in substrate positioning and catalysis shown as sticks and labeled. Note the NLM motif from monomer B, as well as the side chain carboxylate of Glu113′# from monomer C. The side chain phenyl ring of Phe14 in A provides a suitable surface for a stacking interaction with the guanidinium of Arg107 in C, hence contributing to tetramerization. The two substrate molecules shown superimposed on each other have in common an amino group (at positions 4 and 6 in dCyd and dAdo, respectively) and a hydrogen bond acceptor (O2 and N3 in dCyd and dAdo, respectively) which provide anchoring groups for binding to the enzyme

(19.60 kDa). Different oligomeric states are described for different bacterial and protozoan NDTs. On the one hand, NDTs from *Lactobacillus leichmannii*, *L. helveticus*, and *L. reuteri* have been shown to exist as hexamers (showing a molecular weight ranging from 105 to 120 kDa) (Anand et al. 2004; Cook et al. 1990; Fernández-Lucas et al. 2010), whereas type II NDT from *Lactococcus lactis* has been suggested to be a tetramer of 69 kDa (Miyamoto et al. 2007).

## Substrate specificity

To characterize the recombinant *Ct*NDT biochemically and ascribe it to one of the two types of NDTs, we attempted the enzymatic synthesis of nucleosides using different ribo- and 2′-deoxyribonucleosides as donors and several purine and pyrimidine bases as acceptors.

Recombinant *Ct*NDT showed no activity on any of the ribonucleosides tested, namely uridine, cytidine, and adenosine (data not shown). When challenged with 2′-deoxyribonucleosides, *Ct*NDT efficiently cleaved not only those containing purines but also 2′-deoxycytidine, and a similar tendency was observed with respect to the nucleobase acceptors (Table 1).

## Temperature and pH dependence of *Ct*NDT activity

The enzymatic activity of *Ct*NDT was found to be largely preserved (≥ 70%) across a broad temperature range (50–100 °C), with a peak between 60 and 80 °C (Fig. 4a). The pH profile shows that recombinant *Ct*NDT also displays high activity (≥ 70%) in a wide pH range from 3 to 7, with peak values between 5 and 6 (Fig. 4b).

In addition, the effect of temperature on enzyme stability was evaluated by incubating *Ct*NDT over a pH range from 5 to 7 at 70 °C during several days (Fig. 4c). As expected from the dependence of enzyme activity on both temperature and

**Table 1** Production of natural 2′-deoxynucleosides catalyzed by *Ct*NDT

| Specific activity (units/mg protein) | | | | | | |
|---|---|---|---|---|---|---|
| Donor | Acceptor | | | | | |
| | Ade[a] | Gua[b] | Hyp[a] | Cyt[a] | Thy[a] | Ura[a] |
| dAdo | – | n.d. | 27.0 | 7.7 | n.d. | n.d. |
| dGuo | 30.0 | – | 25.0 | 8.0 | n.d. | n.d. |
| dIno | 37.0 | 0.04 | – | 8.8 | n.d. | n.d. |
| dCyd | 12.0 | n.d. | 9.3 | – | n.d. | n.d. |
| dThd | 1.8 | n.d. | 0.7 | n.d. | – | n.d. |
| dUrd | 2.5 | 0.01 | 6.0 | 0.33 | n.d. | – |

*n.d.* not detected

[a] Reaction conditions: 0.6 μg of enzyme in 40 μL at 40 °C, 5 min. [Substrates] = 10 mM, 50 mM MES buffer, pH 6.5

[b] Reaction conditions: 0.6 μg of enzyme in 40 μL at 40 °C, 5 min. [Substrates] = 1 mM in 50 mM phosphate buffer, pH 8.5

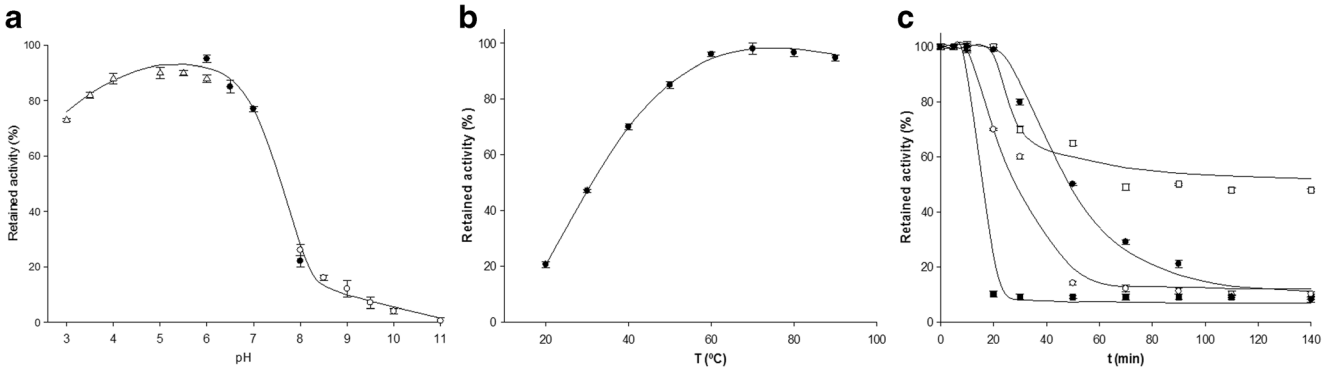


**Fig. 4** Dependence of *Ct*NDT activity and stability on pH and temperature. **a** Effect of pH on *Ct*NDT activity, (empty triangle) sodium acetate 50 mM (pH 3–6), (filled circle) sodium phosphate 50 mM (pH 6–8), (empty circle) sodium borate 50 mM (pH 8–11). **b** Effect of temperature on *Ct*NDT activity. **c** Time course of the thermal inactivation of *Ct*NDT at 60 °C in 10 mM sodium citrate pH 5 (filled square) and pH 6 (filled circle) and in 10 mM sodium phosphate pH 6 (empty square) and pH 7 (empty circle)

pH, our experimental data show that *Ct*NDT is stable over a pH range from 6 to 7 when stored at 60 °C during 25–30 h. Nevertheless, lowering the pH to 5 at 60 °C results in a significant loss of activity after incubation periods longer than 10 h, probably due to irreversible denaturation.

## Effect of organic solvents

We assayed *Ct*NDT activity in the presence of 20% (*v*/*v*) mixtures of water with different water-miscible polar and apolar organic co-solvents, namely glycerol (log $P = -3.03$), ethylene glycol (log $P = -1.80$), DMSO (log $P = -1.3$), *N*,*N*-dimethylformamide (DMF) (log $P = -1.0$), methanol (log $P = -0.76$), propylene glycol (log $P = -0.64$), acetonitrile (log $P = -0.3$), ethanol (log $P = -0.24$), acetone (log $P = -0.21$), isopropanol (log $P = 0.05$), ethyl acetate (log $P = 0.73$), and chloroform (log $P = 1.83$) (Arroyo et al. 2000; Kaul and Banerjee 2008). In most cases (Fig. 5), there was no significant loss of activity, with the important exceptions of glycerol, among the alcohols and polyols, and chloroform, among the apolar solvents.

## Enzymatic production of modified nucleosides

To assess the potential of *Ct*NDT as a biocatalyst, we carried out the enzymatic production of several purine and pyrimidine nucleosides used as APIs, such as didanosine, vidarabine (ara-A), and cytarabine (ara-C), among others (Table 2).

## Molecular modeling

Since *Ct*NDT shows activity toward nucleosides containing either purines or cytosine as donors (Table 1), we built homology models of *Ct*NDT in the apo form and also in the Michaelis complexes with bound dAdo or dCyd (Fig. 3). *Ct*NDT is predicted to have the conserved molecular architecture observed in other NDTs that places the most important base-recognition and catalytic residues in a suitable

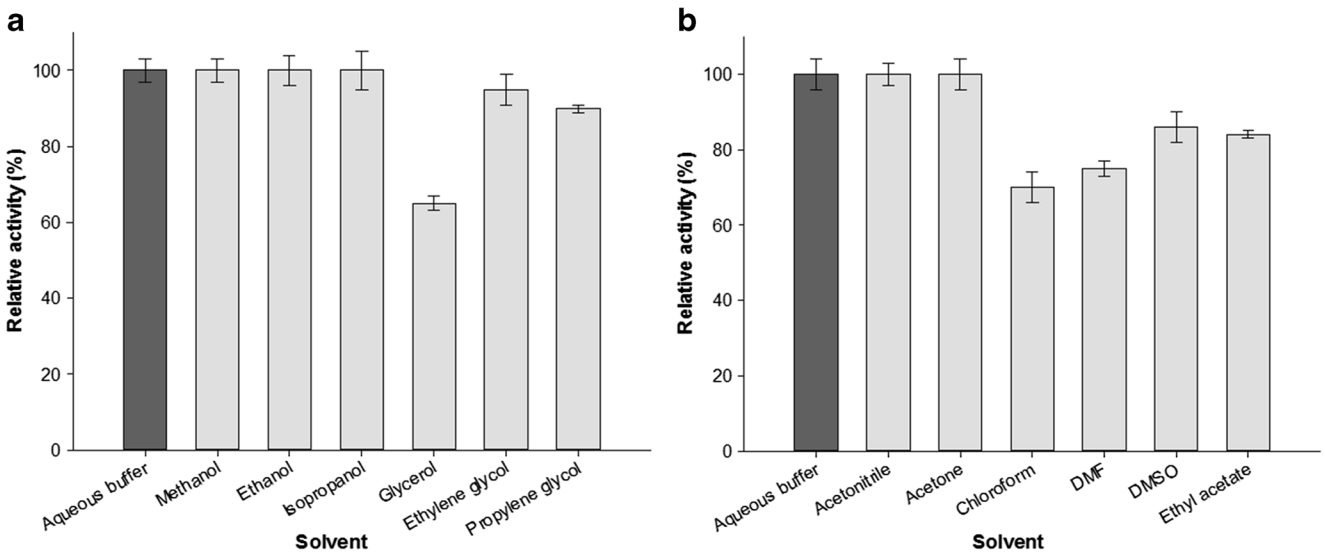


**Fig. 5** Effect of organic co-solvents (20% *v*/*v*) on enzymatic activity of *Ct*NDT. **a** Alcohols and polyols. **b** Aprotic polar solvents

**Table 2** Production (maximum percentage of conversion) of nucleoside analogues catalyzed by *Ct*NDT

| Donor \ Acceptor | Ade[b] | Gua[c] | Hyp[b] | Cyt[b] |
|---|---|---|---|---|
| 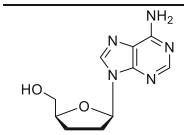 **ddA** | - | 6 | 2.0 | 5 |
| 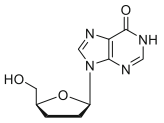 **ddI** | 12 | 3 | - | n.d. |
| 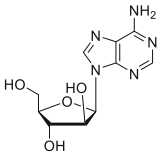 **ara-A** | - | 15 | 4 | 3 |
| 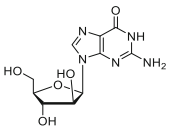 **ara-G** | 14 | - | n.d. | n.d. |
| 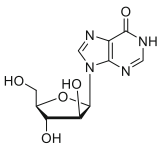 **ara-H** | 9 | 11 | - | n.d. |
| 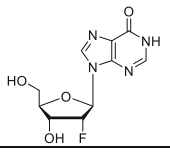 **2'F-Ino** | 11 | 11 | - | n.d |

*n.d.* not detected

[a] Reaction conditions: 3.75 μg of enzyme in 40 μL at 60 °C, 4–24 h. [Substrates] = 1 mM, 50 mM MES buffer, pH 6.5

[b] Reaction conditions: 3 μg of enzyme in 40 μL at 60 °C, 4–24 h. [Substrates] = 1 mM, 50 mM sodium borate 50 mM, pH 8.5

orientation for substrate binding and transition state stabilization. Thus, Glu88, the catalytic residue whose carboxylate attacks the C1′ of the nucleoside, is firmly positioned by the phenol of Tyr7; in the MSA shown in Fig. S3 for crystallographic structures deposited in the Protein Data Bank, replacement by Phe at this position is only seen in the CMP *N*-glycosidase MilB (Sikowitz et al. 2013). The carboxamide nitrogen of Asn118# and the Asp82 carboxylate recognize the O5′ of the 2′-deoxyribose; this aspartate is replaced by a serine in MilB so that it can recognize the 5′-phosphate of CMP instead. Pro11 and Pro40 play a prominent role in making up the active site cavity. The heteroaromatic ring of the nucleobase is sandwiched between the phenyl rings of Phe14 and Phe41 on one side and the hydrophobic side chains of Val58 and Leu119# on the opposite side. The Met120# side chain sulfur appears close to the H1′ atom, which suggests that it likely plays a role in transition state stabilization, together with the carboxylate of Asp62, as seen in the co-crystal structure of CMP-bound MilB (PDB entry 4JEM) (Sikowitz et al. 2013). The side chains of Tyr115′ and possibly Asp53 can establish direct or water-bridged hydrogen bonds with the N7 of purines and the substituent on C6, be it an amino or a keto group. Asp62 of *Ct*NDT is positionally and likely functionally equivalent to Asp78 in MilB, a residue that plays a role in cytosine recognition, together with Arg61 and a protonated Glu62 (Figs. 2 and 3b), which correspond, respectively, to Arg43 and Asn44 in *Ct*NDT.

## Discussion

*Chroococcidiopsis thermalis* is a cyanobacteria, adapted to extremely arid, hot and cold deserts (Billi et al. 2001). Therefore, our expectation that *Ct*NDT would be a hyperthermophilic enzyme that also tolerates acid environments was fulfilled. Indeed, we show that *Ct*NDT presents significant catalytic activity and stability over a wide range of acidic pH values (from 3 to 7) and high temperatures (from 50 to 100 °C). Thus, since no previously reported NDT or PDT has been shown, to the best of our knowledge, to be active in a medium-acid environment or at high temperatures, *Ct*NDT emerges as the first thermostable and acid-tolerant

NDT described so far. The unusual finding that this enzyme can catalyze the transglycosylation reaction using a purine or cytosine as the acceptor base but not uracil or thymine prevents its strict classification as a bona fide type I or type II NDT and hints at the need for an alternative classification scheme.

The ability of *Ct*NDT to recognize also purine nucleosides such as dAdo, dGuo, or dIno as donors must rely on the amino acid composition in the 41–55 region that is often unstructured in most crystal structures of NDTs in the absence of bound substrates. We recently showed that the equivalent region in *Lm*PDT (β2-α3 loop, $^{43}$DNIA$^{46}$) is highly flexible and determines the substrate specificity of this enzyme (Crespo et al. 2017). Therefore, we propose that it is the positionally equivalent region in *Ct*NDT, possibly in conjunction with the backbone carbonyl of Phe49, that allows the recognition of purine bases and cytosine. These rather unique features support the view that the current simplified classification of NDTs may need to be revised and updated in the near future (Crespo et al. 2017).

*Tb*NDT and *Lm*PDT from trypanosomatids have been shown to exist functionally as dimers, whereas *Lh*PDT and *Ll*NDT are hexamers (trimers of dimers). The novel finding that *Ct*NDT is a tetramer, with the only reported precedents being *Lactococcus lactis* NDT (Miyamoto et al. 2007) and the unpublished putative NDT from *Enterococcus faecalis* V583 (PDB entry 3EHD), poses the question of which sequence regions are involved in these differences in multimerization states. Tetramer (A:B-C:D) stabilization in *Ef*NDT is largely driven by (i) the conformation of the $^{75}$DGPTI$^{79}$ loop, which makes up a substantial part of the A-D and B-C dimerization interface at the core of the tetramer; (ii) the $^{102}$TDSR$^{105}$ motif, which provides both the hydroxyl of Thr102 that hydrogen bonds to the NH at the positive end of the $^{13}$QADLRYNAYLVEQIRQ$^{28}$ helix dipole and the arginine (Arg105) that stacks on the phenyl ring of Phe11 in the opposite protomer; (iii) a water-bridged ionic interaction between Arg105 in one subunit, strongly held in place by a buttressing interaction from Asp103, and Asp80 in the opposite subunit; and (iv) additional reciprocal stacking interactions between Ala14:Tyr18, Arg17:Tyr21, Tyr18:Ala14, and Tyr21:Arg17 of subunits A-C and B-D. Remarkably, most of these residues have a clear counterpart in *Ct*NDT (Fig. 3a). Thus, we propose that the $^{77}$NGTPP$^{81}$ loop is located at the core of the *Ct*NDT tetramer and that the guanidinium of Arg107 in the $^{104}$DDFR$^{107}$ motif, buttressed by the carboxylate of Asp105, can both stack on the phenyl ring of Phe14 and make a water-bridged hydrogen bond with Asp82 in the opposite subunit. In addition, the possibility exists that Cys109, which is highly conserved in NDT from cyanobacteria, is involved in an interprotomer disulfide bridge that could play a role in modulating conformational stability and flexibility at high temperatures, as shown for a 5′-deoxy-5′-methylthioadenosine phosphorylase II from the hyperthermophilic archaeon *Sulfolobus solfataricus* (Bagarolo et al. 2015), and/or in providing tolerance to desiccation, as it is known that disulfide bonds can compensate for the destabilizing effect of exposing hydrophobic residues on the protein surface (Linder et al. 2005). Proof of these proposals, however, will have to await the resolution of the crystal structure of the protein and further mutational studies.

Due to the low solubility of some purine bases, such as guanine, xanthine, or other modified purines, the enzymatic synthesis of purine nucleoside analogues from poorly soluble purine bases has been described to be less efficient. To overcome this drawback, many different strategies have been employed, such as raising the pH and/or the temperature (Crespo et al. 2017; De Benedetti et al. 2012; Del Arco et al. 2017; Okuyama et al. 2003; Yokozeki and Tsuji 2000), or adding organic solvents (Fernández-Lucas et al. 2012), and the effect of water-organic co-solvent mixtures on the enzymatic activity and stability of several NDTs has been extensively documented (Castro and Knubovets 2003; Fernández-Lucas et al. 2012). In this regard, several factors such as the denaturing capacity (Khmelnitsky et al. 1991), the polarity index (Gupta et al. 1997), the dielectric constant (Kaul and Banerjee 2008), the log *P* value (Arroyo et al. 2000), and the Dimroth-Reichardt parameter (Moreno and Fágáin 1997) have been considered in general with limited success. For *Ct*NDT, we found that enzymatic activity in the presence of co-solvents is compromised only in the presence of glycerol, chloroform, and DMF (Fig. 5).

Remarkably, glycerol and chloroform are endowed with the most negative and most positive log *P* values, which rules out any linear correlation between hydrophobicity and decreased enzymatic activity. On the contrary, these findings are in good agreement with the common occurrence of glycerol in the active site of several crystallographic structures of NDTs (e.g., 5NBR, 2A0K, 3EHD), where it mimics the 2′-deoxyribose scaffold, and also with the fact that the nucleobase-binding site is mostly hydrophobic (as explained below) and therefore it is expected to show affinity for chloroform. Thus, we propose that the amphipathic nature of the active site provides binding opportunities for these two solvents, and also for DMF, which is also amphipathic and decreases *Ct*NDT activity (Fig. 5), as previously shown for *Lr*NDT (Fernández-Lucas et al. 2012).

Taken together, our results show that *Ct*NDT is, to the best of our knowledge, the first NDT reported to date that is both thermostable and acid tolerant. Moreover, *Ct*NDT displays remarkable activity (80–100%) in the presence of up to 20% of several water-miscible solvents and recognizes not only purine bases and their corresponding 2′-deoxynucleosides as substrates but also, albeit to a lower extent, cytosine and 2′-deoxycytidine. In the light of these findings, the implementation of *Ct*NDT or variants thereof as biocatalysts in an industrial setting could offer a great potential for the synthesis of a

large repertoire of purine and pyrimidine nucleosides, as shown here for the APIs didanosine, vidarabine, and cytarabine.

**Funding** This work was supported by grants SAN151610 from the Santander Foundation and 2017/UEM23 from Universidad Europea de Madrid (to J.F.-L.) and SAF2015-64629-C2-2-R from the Spanish MEC/MICINN (to F.G.).

## Compliance with ethical standards

**Conflict of interest** The authors declare that they have no conflict of interest.

**Ethical approval** This article does not contain any studies with human participants or animals by any of the authors.

## References

Alford RF, Leaver-Fay A, Jeliazkov JR, O'Meara MJ, DiMaio FP, Park H, Shapovalov MV, Renfrew PD, Mulligan VK, Kappel K, Labonte JW, Pacella MS, Bonneau R, Bradley P, Dunbrack RL Jr, Das R, Baker D, Kuhlman B, Kortemme T, Gray JJ (2017) The Rosetta all-atom energy function for macromolecular modeling and design. J Chem Theory Comput 13(6):3031–3048. https://doi.org/10.1021/acs.jctc.7b00125

Anand R, Kaminski PA, Ealick SE (2004) Structures of purine 2′-deoxyribosyltransferase, substrate complexes, and the ribosylated enzyme intermediate at 2.0 Å resolution. Biochemistry 43(9):2384–2393. https://doi.org/10.1021/bi035723k

Armstrong SR, Cook WJ, Short SA, Ealick SE (1996) Crystal structures of nucleoside 2-deoxyribosyltransferase in native and ligand-bound forms reveal architecture of the active site. Structure 4(1):97–107

Arroyo M, Torres-Guzmán R, de la Mata I, Castillón MP, Acebal C (2000) Prediction of penicillin V acylase stability in water-organic co-solvent monophasic systems as a function of solvent composition. Enzym Microb Technol 27(1–2):122–126

Bagarolo ML, Porcelli M, Martino E, Feller G, Cacciapuoti G (2015) Multiple disulfide bridges modulate conformational stability and flexibility in hyperthermophilic archaeal purine nucleoside phosphorylase. Biochim Biophys Acta 1854(10 Pt A):1458–1465. https://doi.org/10.1016/j.bbapap.2015.06.010

Biasini M, Bienert S, Waterhouse A, Arnold K, Studer G, Schmidt T, Kiefer F, Gallo Cassarino T, Bertoni M, Bordoli L, Schwede T (2014) SWISS-MODEL: modelling protein tertiary and quaternary structure using evolutionary information. Nucleic Acids Res 42(Web Server issue):W252–W258. https://doi.org/10.1093/nar/gku340

Billi D, Friedmann EI, Helm RF, Potts M (2001) Gene transfer to the desiccation-tolerant cyanobacterium *Chroococcidiopsis*. J Bacteriol 183(7):2298–2305. https://doi.org/10.1128/JB.183.7.2298-2305.2001

Britos CN, Lapponi MJ, Cappa VA, Rivero CW, Trelles JA (2016) Biotransformation of halogenated nucleosides by immobilized *Lactobacillus animalis* 2′-*N*-deoxyribosyltransferase. J Fluor Chem 186:91–96. https://doi.org/10.1016/j.jfluchem.2016.04.012

Brown PH, Schuck P (2006) Macromolecular size-and-shape distributions by sedimentation velocity analytical ultracentrifugation. Biophys J 90(12):4651–4661. https://doi.org/10.1529/biophysj.106.081372

Case DA, Berryman JT, Betz RM, Cerutti DS, Cheatham TE III, Darden TA, Duke RE, Giese TJ, Gohlke H, Götz AW, Homeyer N, Izadi S, Janowski P, Kaus J, Kovalenko A, Lee TS, LeGrand S, Li P, Luchko T, Luo R, Madej B, Merz KM, Monard G, Needham P, Nguyen H, Nguyen HT, Omelyan I, Onufriev A, Roe DR, Roitberg A, Salomon-Ferrer R, Simmerling CL, Smith W, Swails J, Walker RC, Wang J, Wolf RM, Wu X, York DM, Kollman PA (2015) Assisted model building with energy refinement AMBER 14. University of California, San Francisco

Castro GR, Knubovets T (2003) Homogeneous biocatalysis in organic solvents and water-organic mixtures. Crit Rev Biotechnol 23(3):195–231

Cook WJ, Short SA, Ealick SE (1990) Crystallization and preliminary X-ray investigation of recombinant *Lactobacillus leichmannii* nucleoside deoxyribosyltransferase. J Biol Chem 265(5):2682–2683

Crespo N, Sánchez-Murcia PA, Gago F, Cejudo-Sánches J, Galmes MA, Fernández-Lucas J, Mancheño JM (2017) 2′-Deoxyribosyltransferase from *Leishmania mexicana*, an efficient biocatalyst for one-pot, one-step synthesis of nucleosides from poorly soluble purine bases. Appl Microbiol Biotechnol 101(19):7187–7200. https://doi.org/10.1007/s00253-017-8450-y

De Benedetti EC, Rivero CW, Britos CN, Lozano ME, Trelles JA (2012) Biotransformation of 2,6-diaminopurine nucleosides by immobilized *Geobacillus stearothermophilus*. Biotechnol Prog 28(5):1251–1256. https://doi.org/10.1002/btpr.1602

De Clercq E (2005) Recent highlights in the development of new antiviral drugs. Curr Opin Microbiol 8(5):552–560. https://doi.org/10.1016/j.mib.2005.08.010

Del Arco J, Cejudo-Sánches J, Esteban I, Clemente-Suárez VJ, Hormigo D, Perona A, Fernández-Lucas J (2017) Enzymatic production of dietary nucleotides from low-soluble purine bases by an efficient, thermostable and alkali-tolerant biocatalyst. Food Chem 237:605–611. https://doi.org/10.1016/j.foodchem.2017.05.136

DeLano WL (2013) The PyMOL molecular graphics system. 1.3 edn. Schrödinger, LLC, Portland

Fernández-Lucas J, Acebal C, Sinisterra JV, Arroyo M, de la Mata I (2010) *Lactobacillus reuteri* 2′-deoxyribosyltransferase, a novel biocatalyst for tailoring of nucleosides. Appl Environ Microbiol 76(5):1462–1470. https://doi.org/10.1128/AEM.01685-09

Fernández-Lucas J, Fresco-Taboada A, de la Mata I, Arroyo M (2012) One-step enzymatic synthesis of nucleosides from low water-soluble purine bases in non-conventional media. Bioresour Technol 115:63–69. https://doi.org/10.1016/j.biortech.2011.11.127

Fresco-Taboada A, de la Mata I, Arroyo M, Fernández-Lucas J (2013) New insights on nucleoside 2′-deoxyribosyltransferases: a versatile biocatalyst for one-pot one-step synthesis of nucleoside analogs. Appl Microbiol Biotechnol 97(9):3773–3785. https://doi.org/10.1007/s00253-013-4816-y

Gill SC, von Hippel PH (1989) Calculation of protein extinction coefficients from amino acid sequence data. Anal Biochem 182(2):319–326

Gupta MN, Batra R, Tyagi R, Sharma A (1997) Polarity index: the guiding solvent parameter for enzyme stability in aqueous-organic cosolvent mixtures. Biotechnol Prog 13(3):284–288. https://doi.org/10.1021/bp9700263

Holm L, Laakso LM (2016) Dali server update. Nucleic Acids Res 44(W1):W351–W355. https://doi.org/10.1093/nar/gkw357

Iglesias LE, Lewkowicz ES, Medici R, Bianchi P, Iribarren AM (2015) Biocatalytic approaches applied to the synthesis of nucleoside prodrugs. Biotechnol Adv 33(5):412–434. https://doi.org/10.1016/j.biotechadv.2015.03.009

Kaminski PA (2002) Functional cloning, heterologous expression, and purification of two different *N*-deoxyribosyltransferases from *Lactobacillus helveticus*. J Biol Chem 277(17):14400–14407. https://doi.org/10.1074/jbc.M111995200

Kaminski PA, Dacher P, Dugue L, Pochet S (2008) *In vivo* reshaping the catalytic site of nucleoside 2′-deoxyribosyltransferase for dideoxy- and didehydronucleosides via a single amino acid substitution. J

Biol Chem 283(29):20053–20059. https://doi.org/10.1074/jbc.M802706200

Kaul P, Banerjee UC (2008) Predicting enzyme behavior in nonconventional media: correlating nitrilase function with solvent properties. J Ind Microbiol Biotechnol 35(7):713–720. https://doi.org/10.1007/s10295-008-0332-y

Kelley LA, Mezulis S, Yates CM, Wass MN, Sternberg MJ (2015) The Phyre2 web portal for protein modeling, prediction and analysis. Nat Protoc 10(6):845–858. https://doi.org/10.1038/nprot.2015.053

Khmelnitsky YL, Mozhaev VV, Belova AB, Sergeeva MV, Martinek K (1991) Denaturation capacity: a new quantitative criterion for selection of organic solvents as reaction media in biocatalysis. Eur J Biochem 198(1):31–41

Laemmli UK (1970) Cleavage of structural proteins during the assembly of the head of bacteriophage T4. Nature 227(5259):680–685

Lapponi MJ, Rivero CW, Zinni MA, Britos CN, Trelles JA (2016) New developments in nucleoside analogues biosynthesis: a review. J Mol Catal B Enzym 133:218–233. https://doi.org/10.1016/j.molcatb.2016.08.015

Lawrence KA, Jewett MW, Rosa PA, Gherardini FC (2009) *Borrelia burgdorferi* bb0426 encodes a 2′-deoxyribosyltransferase that plays a central role in purine salvage. Mol Microbiol 72(6):1517–1529. https://doi.org/10.1111/j.1365-2958.2009.06740.x

Lewkowicz E, Iribarren A (2006) Nucleoside phosphorylases. Curr Org Chem 10(11):1197–1215. https://doi.org/10.2174/138527206777697995

Linder MB, Szilvay GR, Nakari-Setala T, Penttila ME (2005) Hydrophobins: the protein-amphiphiles of filamentous fungi. FEMS Microbiol Rev 29(5):877–896. https://doi.org/10.1016/j.femsre.2005.01.004

López-Blanco JR, Canosa-Valls AJ, Li Y, Chacón P (2016) RCD+: fast loop modeling server. Nucleic Acids Res 44(W1):W395–W400. https://doi.org/10.1093/nar/gkw395

Mikhailopulo I (2007) Biotechnology of nucleic acid constituents—state of the art and perspectives. Curr Org Chem 11(4):317–335. https://doi.org/10.2174/138527207780059330

Mitsukawa Y, Hibi M, Matsutani N, Horinouchi N, Takahashi S, Ogawa J (2017) Enzymatic synthesis of 2′-O-methylribonucleosides with a nucleoside hydrolase family enzyme from *Lactobacillus buchneri* LBK78. J Biosci Bioeng 123(6):659–664. https://doi.org/10.1016/j.jbiosc.2017.01.005

Miyamoto Y, Masaki T, Chohnan S (2007) Characterization of *N*-deoxyribosyltransferase from *Lactococcus lactis* subsp. *lactis*. Biochim Biophys Acta 1774(10):1323–1330. https://doi.org/10.1016/j.bbapap.2007.08.008

Moreno J, Fágáin CO (1997) Activity and stability of native and modified alanine aminotransferase in cosolvent systems and denaturants. J Mol Catal B Enzym 2(6):271–279. https://doi.org/10.1016/s1381-1177(96)00018-5

Okuyama K, Shibuya S, Hamamoto T, Noguchi T (2003) Enzymatic synthesis of 2′-deoxyguanosine with nucleoside deoxyribosyltransferase-II. Biosci Biotechnol Biochem 67(5):989–995. https://doi.org/10.1271/bbb.67.989

Oliva C, Sánchez-Murcia PA, Rico E, Bravo A, Menéndez M, Gago F, Jiménez-Ruiz A (2017) Structure-based domain assignment in *Leishmania infantum* EndoG: characterization of a pH-dependent regulatory switch and a C-terminal extension that largely dictates DNA substrate preferences. Nucleic Acids Res 45(15):9030–9045. https://doi.org/10.1093/nar/gkx629

Parker WB (2009) Enzymology of purine and pyrimidine antimetabolites used in the treatment of cancer. Chem Rev 109(7):2880–2893. https://doi.org/10.1021/cr900028p

Patel RN (2017) Biocatalysis for synthesis of pharmaceuticals. Bioorg Med Chem 26:1252–1274. https://doi.org/10.1016/j.bmc.2017.05.023

Salomon-Ferrer R, Götz AW, Poole D, Le Grand S, Walker RC (2013) Routine microsecond molecular dynamics simulations with AMBER on GPUs. 2. Explicit solvent particle mesh Ewald. J Chem Theory Comput 9(9):3878–3888. https://doi.org/10.1021/ct400314y

Sikowitz MD, Cooper LE, Begley TP, Kaminski PA, Ealick SE (2013) Reversal of the substrate specificity of CMP N-glycosidase to dCMP. Biochemistry 52(23):4037–4047. https://doi.org/10.1021/bi400316p

Somervuo P, Holm L (2015) SANSparallel: interactive homology search against Uniprot. Nucleic Acids Res 43(W1):W24–W29. https://doi.org/10.1093/nar/gkv317

Van Holde KE (1985) Physical biochemistry, 2nd edn. Prentice-Hall, Englewood Cliffs

Vichier-Guerre S, Dugué L, Bonhomme F, Pochet S (2016) Expedient and generic synthesis of imidazole nucleosides by enzymatic transglycosylation. Org Biomol Chem 14(14):3638–3653. https://doi.org/10.1039/c6ob00405a

Yokozeki K, Tsuji T (2000) A novel enzymatic method for the production of purine-2′-deoxyribonucleosides. J Mol Catal B Enzym 10(1–3):207–213. https://doi.org/10.1016/s1381-1177(00)00121-1